Journal of University of Science and Technology Beijing
Volume 9, Number 3, June 2002, Page 197

Materials

Capacity fading of spinel $LiMn_2O_4$ during cycling at elevated temperature

Yanbin Chen and Qingguo Liu

Laboratory of Solid State Ionics, University of Science and Technology Beijing, Beijing 100083, China
(Received 2001-09-20)

Abstract: A normal spinel $LiMn_2O_4$ as cathode material for lithium-ion cells was cycled galvanostatically (0.2 C) at 55℃. To determine the contribution of each voltage plateau to the total capacity fading of the cathode upon repeated cycling, the capacities in each plateau were separated by differentiation of voltage *vs.* capacity. The results show that the capacity fading in the upper voltage plateau is more rapidly than that in the lower during discharging, while in charging process, it fades slower than that in the lower voltage range. The increased capacity shift and aggravated self-discharge/electrolyte oxidation during discharging contribute to a high fading rate in the upper step. Capacity shift also takes place during charging process, which again enhancing the fading rate of the lower voltage plateau. An increase in capacity shift, as a result of an increase in polarization of the cell, plays a major role in determining the fading rate in each voltage plateau, further reflecting the thickening of the passivation layer on the active particles, and the accumulation of electrolyte decomposition. The relative capacity loss for modified spinels is well correlated with the relative increase in the polarization of the half-cells, confirming the above causes for capacity fade of this kind of cathode material.

Key words: spinel $LiMn_2O_4$; capacity fading; capacity shift; self-discharge; lithium reinsertion; electrolyte oxidation

1 Introduction

Spinel $LiMn_2O_4$ is extensively recognized as a promising cathode candidate for lithium ion batteries by virtue of its low cost, low toxicity and high electrochemical potential. Its fairly good safety attribute makes it more attractive for large-sized batteries as a traction power for electric vehicle (EV) and hybrid electric vehicle (HEV) or as stationary energy storage devices. However, $LiMn_2O_4$ suffers from rapid capacity fading during cycling or storage, especially at elevated temperature, a drawback stands in its industrial application.

The mechanism for capacity fading of spinel $LiMn_2O_4$ during cycling or storage has been investigated by many researchers. The causes for the failure of the material reported so far in the literature [1-8] is summarized as: (1) dissolution of Mn from the spinel matrix, and thus induced structural change, (2) fracture of particles due to repeated cycling, (3) formation of passivating film, (4) Jahn-Teller effect and (5) decomposition of the electrolytes.

Nevertheless, it still remains controversial in some aspects. First, the results on fading rate within the two potential plateaus are not well agreed with each other. Xia *et al.* [6] reported that capacity fading in the upper voltage plateau dominates the total fading process both at ambient and high temperature due to the transformation of unstable two-phase to a more stable one-phase structure; on the other hand, Robertson *et al.* [7] and Huang *et al.* [8] reported that the capacity loss mainly takes place in lower voltage step where the concentration of Mn (III) is significant and thus its dissolution; whereas Nishimura *et al.* [11] stated that the capacity fade in each voltage plateau is comparable. Second, Thackery *et al.* [9] and Liu *et al.* [10] provided evidences of Jahn-Teller effect for spinel $LiMn_2O_4$ cathode cycled at room temperature due to kinetic polarization, but there is no report up to now in this respect at high temperature. Finally, the effect of electrolyte decomposition on capacity fading is not clearly defined.

A spinel $LiMn_2O_4$/Li half-cell was cycle at 55℃, and the cycling capacities in each voltage plateau were separated and compared, in order to make out their contributions to the capacity fade and the related causes. The results are reported in this paper.

2 Experimental

The spinel $LiMn_2O_4$ was synthesized *via* solid state reaction. The starting materials Li_2CO_3, and electrolytic MnO_2 were weighed according to the nominal composition, and then thoroughly mixed by ball-milling. The uniformly mixed precursors were sintered at 800℃ in air for 40 h with intermittent grinding, and cooled to room temperature at a slow rate of 0.2 ℃/min.

Powder X-ray diffraction was performed for the synthesized spinel to detect phase purity using a Rigaku

Corresponding author: Yanbin Chen **E-mail**: chen-yb@richlandhkg.com.hk

diffractometer with a graphite-filtered Cu-K_α radiation. The diffraction patterns were taken at room temperature in the range of $15°<2\theta<90°$ using step scans. The step size was 0.02°.

Electrochemical performance of the spinel as cathode material was evaluated in a prototype cell containing Li foil in excess as anode. The composite cathode was a mixture (mass fraction) of 85% active material, 10% acetylene black, and 5% PTFE binder. The cathode was vacuum-dried at 140℃ for 24 h before being assembled into the test cell. The electrolyte 1 mol/L $LiPF_6$/Ethylene carbonate-dimethyl carbonate (EC-DMC 1:1 in volume) was used as received from Merck, and Celgard 2400 film as separator. All the cells were assembled in a glove-box filled with flowing dry-air. The cell was assembled in a glove-box filled with the flowing dry-air, and then placed in a thermostat of (55 ± 0.5)℃ when cycling at a constant current of 0.2C between 3.4-4.35 V.

3 Results and discussion

The X-ray diffractometry of the as-prepared sample was conducted. All the peaks are indexed to cubic spinel phase (space group Fd3m), and no additional peaks for impurities are observed. Moreover, the relative peak intensities are similar to those of $LiMn_2O_4$. These indicate that the sample has a normal spinel structure.

The cycleability of the half-cell containing the spinel as cathode was evaluated by galvanostatic charge/discharge at 0.2C in a thermostat of 55℃. The typical charging/discharging curves in several cycles are shown in **figure 1**. Both the charge and discharge capacities steadily decrease through 50 cycles, respectively remaining about 72.4% and 75.5% of their initial values. Besides, the coulombic efficiency slightly decreases from 97.4% to 97%, although it remains steadily at about 100% when cycling at room temperature.

To identify the contribution of each plateau to the total capacity fading, the operating voltage of the half-cell in each cycle was differentiated by capacity, *i.e.* dV/dC (V—voltage, C—capacity). Plotting of dV/dC *vs.* C gives the capacity data of both plateaus (as shown at the peak in **figure 2**) with an uncertainty of $\leqslant\pm0.3$ mAh/g [11], thus the reproducible capacity value in each plateau can be obtained.

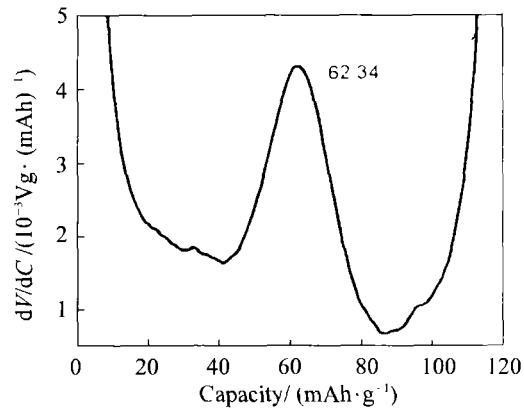

Figure 2 Plot of dV/dC *vs* capacity to separate the capacities in each plateau (at about 3.95 V and 4.05 V respectively).

Figure 3 and **figure 4** show the charge/discharge capacities, and cycling efficiencies of the two voltage steps. Two interesting features in figure 3 can be observed. First, The initial capacity in charging process is much larger than that in the discharging, thus giving an very low cycling efficiency, which accounts for the formation of the passivation film on the surface of active particles. In other words, it is not in the high voltage plateau but the low voltage range that the passivating film is formed. As another feature, although the discharge capacity (Q_{d-1}) is much lower than the charge

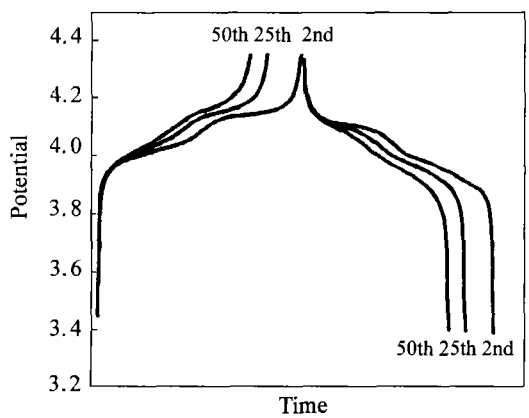

Figure 1 Evolution of charging/discharging curves with cycle number.

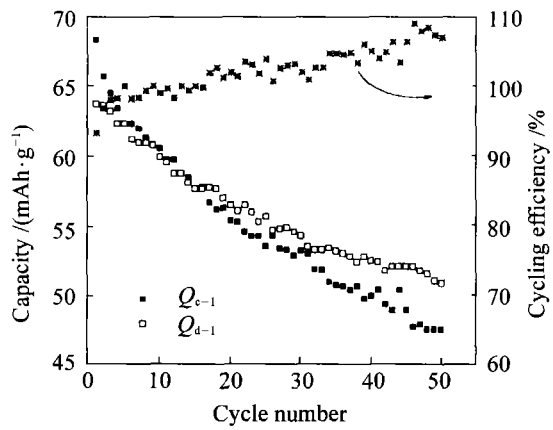

Figure 3 Variation of charge/discharge capacities in the lower voltage plateau, and the change of cycling efficiency with cycle number.

capacity (Q_{c-1}) at the initial stage, it decreases slowly and then surpasses Q_{c-1} after the 14th cycle, and the gap between them becomes increasingly large at extended cycling. Correspondingly, the cycling efficiency increases steadily even over 100%. This is quite different from the general case for a cell's cycling, which clearly indicates that a certain amount of capacity shifts from the upper voltage step to the other during discharging, and *vice versa*. The slope of curve, *i.e.* dV/dC, in upper voltage step is smaller than that in the lower step, thus the capacity shift during discharging will be larger than that in the charging process.

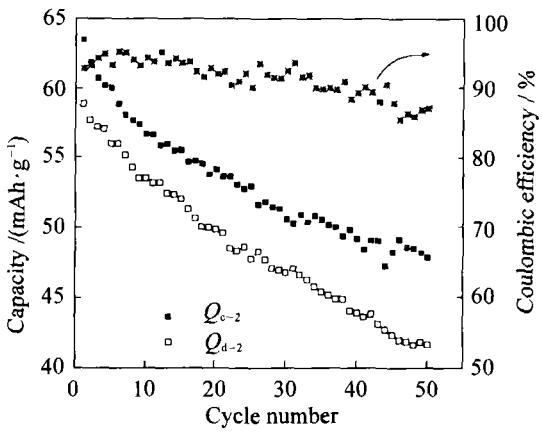

Figure 4 Variation of charge/discharge capacities in the upper voltage plateau, and the change of cycling efficiency with cycle number.

In the upper voltage plateau (figure 4), the discharge capacity (Q_{d-2}) remains normally low relative to the charge capacity (Q_{c-2}), and decreases more quickly. Consequently, the gap between them becomes more significant upon cycling, and the cycling efficiency decreases greatly. Besides the capacity shift to the low cycling efficiency, another potential factor resulting in the low cycling efficiency is the electrolyte oxidation. Although $LiPF_6$/EC-DMC with optimized composition can be safely used for lithium cells at a voltage of $\leqslant$4.9 V at room temperature and 4.7 V at 55℃ [12], but it still undergoes decomposition at a discernibly low rate even within the safe voltage limit. Aurbach *et al.* [13] also found that EC-DMC (1:3) begins to be oxidized at 3.7 V at room temperature, although the reaction rate is slow in the voltage range of 3.7-4.2 V. Undoubtedly, the electrolyte oxidation will be enhanced at high temperature. That's why the cycling efficiency (at about 97.4%) at 55℃ of the cell is lower than that at roo m temperature (at about 100%) in the experiment conditions of present case. Electrolyte oxidation was evidenced in several occasions where the glass cell-case was broken due to the increase of internal pressure. Electrolyte oxidation has an effect on the cycling efficiency. It consumes some capacity at the end of charging, contributing to the apparent charge capacity; in the discharging process, it also takes place in the same voltage range, which can electronically compensate for lithium reinsertion reaction (self-discharge) [5], causing a decrease in discharge capacity, and thus lowering the cycling efficiency. The more serious are the electrolyte oxidization and the self-discharge, the lower is the cycling efficiency. Another effect of electrolyte oxidation is the accumulative decrease in ionic conductivity, which leads to an increase in polarization of the cell.

Figure 5 compares the cycling stability of the two voltage steps during discharging at high temperature. The discharge capacity in the upper voltage range (Q_{d-2}) is smaller and fades more quickly than that in the lower range (Q_{d-1}).

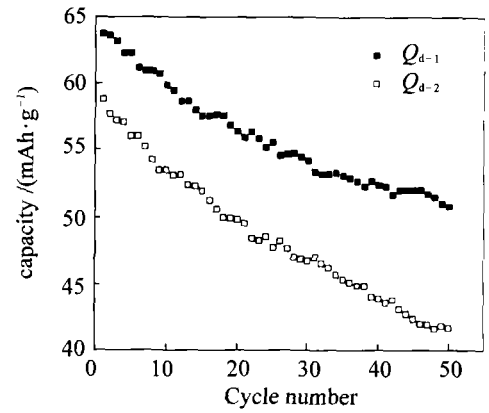

Figure 5 Variation of discharge capacity in the two voltage plateaus.

The loss of active mass due to particle fracture at repeated intercalation/deintercalation, if any, is supposed to have nearly a same effect on the capacity loss in the two successive voltage steps [4,14,15]; so does the degradation of the electrolyte conductivity. Also, the manganese dissolution during the charging process [4] will not cause any difference in the Mn-content of the particles in both steps. Therefore, the difference in the fading rate of the two voltage plateaus may result from two possible factors as follows. The first is that the capacity shift from the upper voltage plateau to the other becomes gradually large due to the increasing polarization of the half-cell, as the result of thickening of the passivating layer on the active mass and cumulated electrolyte oxidation [1-3]. The other is the side reaction like the electrolyte oxidation/lithium-reinsertion during discharging, as discussed above. This is supported by Huang *et al.* [8], although the storage properties of spinel $LiMn_2O_4$ at various state of charge (SOC) were evaluated in their experiment. They concluded that the reversible lithium reinsertion is a dominant mechanism of chemical instability for charged electro-

des at elevated temperature; even in discharged state at room temperature, the reinsertion may contribute at least as much to capacity loss as does Mn dissolution. The slight decrease in the cycling efficiency of the cell indicates the intensifying of the side reaction in the upper voltage plateau in extended cycling, due to an increase in specific area as a result of particle fracture [4,14,15] and thickening of passivating layer.

Figure 6 gives the charge capacities in the two voltage plateaus, Q_{c-1} and Q_{c-2}, respectively. Q_{c-2} fades slowly compared with Q_{c-1}, which seems to be contradicted with the data in figure 5. This reminds of capacity shift, which also takes place in the charging process, although it is expected to be lower than that in the discharging process due to the lager slope of dV/dC in plateau 1 than in plateau 2. The capacity shift from plateau 1 to plateau 2 also increases with the cycle number, therefore, Q_{c-1} declines more rapidly.

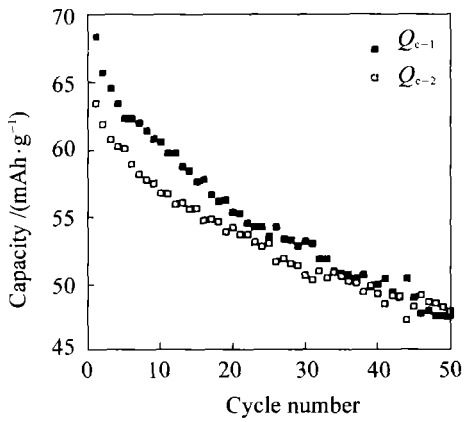

Figure 6 Variation of the charge capacity in the two voltage plateaus.

Worthy of mentioning, the results by Xia *et al.* [6] and Nishimura *et al.* [11] were different from those of present work. Xia *et al.* [6] reported that the capacity fade in the upper voltage plateau dominates the whole fading process by comparing the plateau length of charge curves in different cycles. But the shape of the voltage plateaus and the boundary between them become less distinctly with the increase in cycle number (see figure 1), hence, errors could be involved. Nishimura *et al.* [11] also separate the capacities in both voltage plateaus in the charging curves after the cathode soaked in the electrolyte, which stored at high temperature and different duration, and they concluded that the fading rate in the two plateaus is comparable. However in their experiments, the upper cut-off voltage (4.3 V) is not high enough to extract all the reversible Li^+ ions due to the increased polarization as a result of the extension of storage duration. If considering these residual Li^+ ions, the fading rate in the lower voltage plateau would be faster, which well coincide with the results of present work.

The relationship of the fading rate in each plateau with the increase in polarization of the half-cell was discussed above. In fact, the evolution of the polarization of the half-cell can be clearly seen from the cycling curves of the 2nd, 25th and 50th cycle in figure 1. The charging voltage increases and the discharging voltage decreases, and therefore the polarization increases with extended cycling. **Figure 7** shows more clearly this point. The average charging voltage increases while the average discharging voltage decreases with the cycle number, correspondingly, the difference between them increases, which well reflects the exacerbation of the polarization of the half-cell.

From the above discussion, it can be concluded that the polarization increase of the cell and thus the increase in the capacity shift determine the relative fading rate in the two successive plateaus. As an extrapolation, it is expected that the polarization increase would also correspond to the relative fading of various modified spinel lithium manganese oxides. **Figure 8** gives the evolution of the average voltage difference of

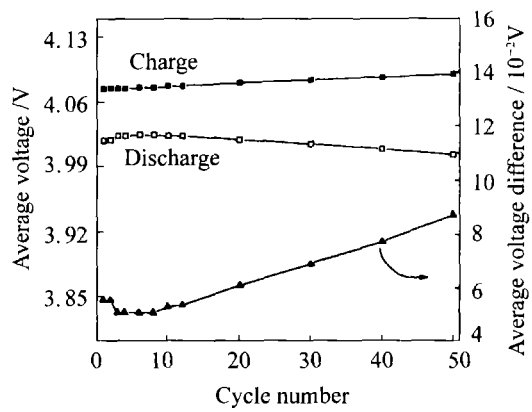

Figure 7 Variation of average voltage in charge/discharge of half-cell $Li/LiMn_2O_4$, and change of average voltage difference with cycle number.

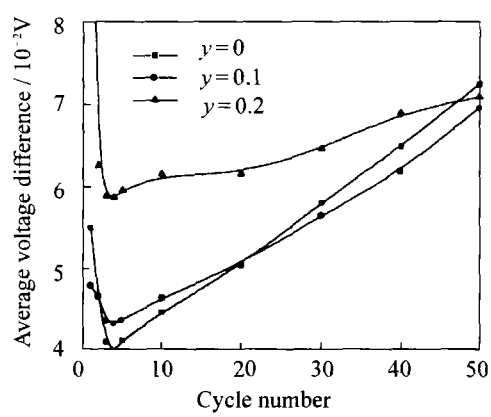

Figure 8 Variation of average voltage difference of half-cell $Li/Li_{1.05}Mn_{2-y}Cr_yO_4$ (y=0, 0.1, 0.2) with cycle number.

the half-cells containing Cr-doped spinels LiMn $LiMn_{2-y}Cr_yO_4$ ($y=0, 0.1, 0.2$) as cathodes with the cycle number. The average voltage difference decreases during the initial cycles, and then increases significantly. By comparison, the polarization of the spinel with a high Cr-doping level increases at a low rate, which correlates well with a low fading rate. With increasing Cr-doping content, the dissolution of the cathode and the thickening of the passivation layer are suppressed, therefore the polarization of the half-cell increases less.

4 Conclusion

By analyzing the cycling behaviors of spinel $LiMn_2O_4$ and modified spinels at high temperature, the mechanism for capacity fading of this kind of cathode material is clarified, which can be summarized as follows:

(1) The contributions of each voltage plateau during charge/discharge to the total fading of spinel are clearly figured out. The capacity fading in the upper voltage range is more rapidly than that in the lower during discharging, while in charging process, it fades slower than that in the lower voltage plateau.

(2) The increased capacity shift, as a result of increased polarization of the cell, plays a major part in determining the fading rate in each voltage plateau. The more capacity shift takes place, the more significant difference in fading rate between voltage plateaus.

(3) Spinels with different composition or from different preparation procedure demonstrate different cycling behavior. The increase in the polarization of the half-cell with various modified spinel $LiMn_2O_4$ cathode is well correlated to the magnitude of capacity fade.

References

[1] A. Blyr, C. Sigala, G.G. Amatucci, D. Guyomard, Y. Chabre, and J.M. Tarascon, Self-discharge of $LiMn_2O_4$/C Li-ion cells in their discharged state [J], *J. Electrochem. Soc.*, 145(1998), p.194.

[2] A.D. Pasquier, A. Blyr, P. Courjal, D. Larcher, G. Amatucci, B.Gerand, and J.M. Tarascon, Mechanism for limited 55℃ storage performance of $Li_{1.05}Mn_{1.95}O_4$ electrodes [J], *J. Electrochem. Soc.*, 146(1999), p.428.

[3] A.D. Pasquier, A. Blyr, A. Cressent, C. Lenain, G. Amatucci, and J.M. Tarascon, An update on the high temperature ageing mechanism in $LiMn_2O_4$-based Li-ion cells [J], *J. Power Sources*, 81-82(1999), p.54.

[4] D. Song, H. Ikuta, and M. Wakihara, Cyclability and dissolution of manganese in substituted stoichiometric and non-stoichiometric lithium manganese oxides at high temperature [J], *Electrochemistry*, 68(2000), p.460.

[5] D. Guyomard, J.M. Tarascon, The carbon/$LiMn_2O_4$ system [J], *Solid State Ionics*, 69(1994), p.222.

[6] Y. Xia, Y. Zhou, and M. Yoshio, Capacity fading on cycling of 4V Li/$LiMn_2O_4$ cells [J], *J Electrochem Soc*, 144(1997), p. 2593.

[7] A.D. Robertson, S.H. Lu, and W.F. Howard, M^{3+}-modified $LiMn_2O_4$ spinel intercalation cathodes [J], *Jr. J. Electrochem. Soc.*, 144(1997), p.3505.

[8] H. Huang, C.A. Vincent, and P.G. Bruce, Capacity loss of lithium manganese oxide spinel in $LiPF_6$/EC-DMC electrolytes [J], *J. Electrochem. Soc.*, 146(1999), p.481 .

[9] M.M. Thackery, S.H. Yang, A. Kahaian, K.D. Kepler,E. Skinner, J.T. Vaughey, and S.A. Hackney, Structural fatigure in spinel electrodes in high voltage (4V) Li/$LiMn_2O_4$ cells [J], *Electrochem. Solid-State Letters*, 1998, No.1, p.7.

[10] W. Liu, K. Kowal, and G.C. Farrington, Electrochemical characteristic of spinel phase $LiMn_2O_4$-based cathode materials prepared by the Pechini process [J], *J. Electrochem. Soc.*, 143(1996), p.3590.

[11] K. Nishimura, T. Douzono, M. Kasai, H. Ando, Y. Muranaka, and Y. Kozono, Spinel-type lithium manganese oxide cathodes for rechargeable lithium batteries [J], *J. Power Sources*, 81-82(1999), p.420.

[12] J.M. Tarascon and D. Guyomard, New electrolyte composition stable over the 0 to 5V voltage range and compatible with the $Li_{1-x}Mn_{2-x}O_4$/carbon Li-ion cells [J], *Solid State Ionics*, 69(1994), p.293.

[13] D. Aurbach, M.D. Levi, K. Gamulski, B. Markovsky, G. Salitra, E. Levi, U. Heider, L. Heider, and R. Oesten, Capacity fading of $LiMn_2O_4$ spinel electrodes studed by XRD and electroanalytical techniques [J], *J. Power Sources.*, 812 (1999), p.472.

[14] T. Ohzuku, H. Tomura, and K. Sawai, Monitoring of particle fracture by acoustic emission during charge and discharge of Li/MnO_2 cells [J], *J. Electrochem. Soc.*, 144(1997), p.3496.

[15] K. Dokko, M. Nishizawa, S. Horikoshi, T. Itoh, M. Mohamedi, and I. Uchida, In situ observation of $LiNiO_2$ single-particle fracture during Li-ion extraction and insertion [J], *Electrochem. Solid-State Letters*, 2000, No.3, p.125.